Grant-Free Access in Multi-Cell Massive MIMO through Learning Cooperative Activity Detection over Riemannian Manifolds

Rashed Shelim and Ahmed S. Ibrahim
Department of Electrical and Computer Engineering, Florida International University, Miami, USA
rshel019@fiu.edu, aibrahim@fiu.edu

***Abstract*—Grant-free (GF) or random access is a key enabler for low-latency massive machine-type communications (mMTC), where devices are sporadically active and transmit small amounts of data. Massive multiple-input multiple-output (mMIMO) technology can enable users' activity detection for such random access, due to its inherent spatial diversity. One approach employs the sample covariance matrices of received signals to estimate the activity detection. Such covariance-based schemes utilize sub-optimal search algorithms (e.g., coordinate-wise gradient descent) to find solutions for the non-convex maximum likelihood (ML) estimation problem of user activity detection. Covariance matrices are symmetric positive definite (SPD) ones and hence they can be represented over Riemannian manifolds (i.e., curved surfaces). Consequently, users can be represented over such non-Euclidean manifold using a combination of the sufficient-statistic sample covariance matrices and user-dependent pilot sequences. Such unique user's modeling over Riemannian manifolds paves the road to use geometric-based solutions for activity detection. Specifically in this paper, we propose to utilize geometric k-means clustering to divide users of multi-cell massive MIMO system into two distinct groups, namely, active and inactive ones. Geodesic distances among users' representations over Riemannian manifold are measured using log-determinant Bregman divergence. Simulation results show that the proposed method reduces probability of miss detection compared to Euclidean-based state-of-the-arts. Finally, the proposed method requires less complexity than Euclidean ones.**

***Index Terms*—Activity detection, grant-free access, log-determinant Bregman Divergence, Riemannian manifolds, symmetric positive definite matrices.**

I. Introduction

Next-generation wireless systems aim to offer widespread connectivity to numerous Internet-of-Things (IoT) devices and massive machine-type communication (mMTC) [1]. Unlike human-to-human communication, mMTC is characterized by three primary attributes, which are massive connectivity, sporadic traffic pattern, and short data packets. Conventional grant-based access scheme requires excessive signaling overhead to allocate time-frequency resources for devices with pending uplink transmissions. As a result, grant-based access scheme causes high latency on the control plane (CP), which is not suitable for some IoT services with ultra-reliable low-latency communications (URLLC) requirements such as industrial IoT (e.g., factory automation). To achieve *low-latency* communication, a grant-free (GF), or random, access scheme has been proposed as an alternative solution [1], [2].

This work was supported in part by the National Science Foundation under Award CNS-2144297.

One of the main challenges facing GF access in massive MIMO (mMIMO) systems is *users' activity detection,* which aims to identify the group of active users or devices with uplink transmission in any given time slot. Recently, two major approaches have been proposed for user's activity detection. On one hand, the activity detection problem was formulated as a compressed sensing (CS) one, which takes advantage of the sporadic traffic nature in many mMTC use cases, and was solved using various CS approaches such as approximate message passing (AMP) [2]. On the other hand, *covariance-based* approaches were proposed for user activity detection, which utilized sample covariance matrices of the received signals over Euclidean domain [1], [3], [4]. A generalization for covariance-based approaches to multi-cell MIMO systems was considered in [5], [6]. However, such covariance-based schemes utilize sub-optimal search algorithms (e.g., coordinate-wise gradient descent) to solve the *non-convex* maximum likelihood (ML) estimation problem of activity detection [7]. In searching for a better and *lower-complexity* solution, we consider the mathematical framework of *Riemannian geometry* in this paper as follows.

Sample covariance matrices of received signals at a given base station can be modeled over Riemannian manifolds (i.e., curved surfaces), thanks to being symmetric positive definite (SPD) [8]–[11]. Such modeling paves the road for non-Euclidean geometric-based solution of activity detection problem. To this end, we focus on multi-cell mMIMO system, which includes multiple base stations that are connected to a central unit (e.g., in C-RAN). Users are assigned distinctive, but *non-orthogonal,* pilot sequences. As the sample covariance matrix at each base station is a sufficient statistic for activity detection, each user is represented using an SPD signature which is a combination of the received sample covariance matrix and its pilot sequence. A geodesic distance, such as log-determinant Bregman divergence, is used to measure the geodesic distance among users' signatures over the manifold.

In this paper and based on such geometric modeling of users, we propose a *cooperative activity detection* scheme, where we utilize k-means clustering to divide the users' signatures over Riemmanian manifold into two groups, active and inactive users. The group of active users represent the solution to the activity detection problem across multiple cells. Simulation results demonstrate that the proposed geometric approach *reduces the probability of miss detection* compared to

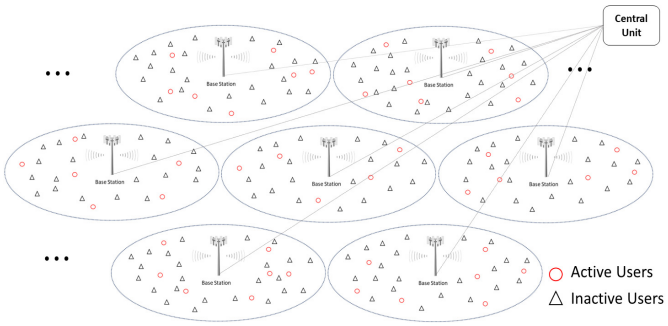

Fig. 1: Grant-free access in uplink multi-cell mMIMO systems.

Euclidean-based state-of-the-arts and effectively works in both singe-cell and multi-cells scenarios. Equally important and despite the proposed method being non-Euclidean in nature, it is *less computationally complex* than Euclidean-baed ones.

The rest of this paper is organized as follows. The system model is presented in Section II. Section III discusses the problem formulation of activity detection over Riemannian manifolds. Section IV presents the proposed learning-based user activity detection solution. Simulation results are presented in Section V. Finally, Section VI presents the conclusion.

II. System Model

In this section, we provide an overview on Riemannian geometry, then we present the multi-cell network model.

A. Riemannian Manifolds and Bregman divergence

A differentiable manifold $\mathcal{M}$ is a topological space [12] where each point p has a neighborhood that is topologically equivalent to a Euclidean space. The tangent space $T_p\mathcal{M}$ at any point $p \in \mathcal{M}$ is a set of tangent vectors which are the derivatives of curves passing through the point p. A Riemannian manifold $(\mathcal{M}, g_p)$ is a smooth and real manifold $\mathcal{M}$ equipped with a positive definite inner product g_p at each point p on the tangent space $T_p\mathcal{M}$ and is studied via Riemannian geometry [12]. An $n \times n$ SPD matrix is represented over the interior of cone-like manifold $\mathcal{S}^n_{++} := \{\mathbf{P} \in \mathbb{R}^{n\times n} | \mathbf{P} = \mathbf{P}^T, \mathbf{P} \succ 0\}$, which is a special class of Riemannian manifolds [13]. A function is of Bregman type if it possesses the characteristics of strict convexity, continuous differentiability, and bounded level sets [14]. The Bregman divergence for any strictly positive definite matrices $\mathbf{P}, \mathbf{Q} \in \mathcal{S}^n_{++}$ is computed via the log-determinant Bregman function [15], which is given by

$$\mathcal{D}(\mathbf{P}\|\mathbf{Q}) = -\log\det\mathbf{P} + \log\det\mathbf{Q} + \langle\langle \mathbf{Q}^{-1}, \mathbf{P}-\mathbf{Q}\rangle\rangle, \quad (1)$$

where $\langle\langle , \rangle\rangle$ denotes the trace inner product of SPD matrices.

B. Network and Channel Models

We consider an uplink multi-cell system, as shown in Fig. 1, which consists of B neighboring cells with M antennas at each base station and N single-antenna users at each cell. Moreover, we consider cooperation among the B base stations, as they are assumed to be connected to a central unit. Uplink signals, transmitted by active users, are collected through their designated stations and jointly processed at such central unit.

Given the sporadic traffic of many mMTC services, only a small number $K_c \ll N$ of users in each cell are active in each coherence block. Each user k, $k = 1, 2, \cdots, N$, in cell b, $b = 1, 2, \cdots, B$ is given a pilot sequence, which is a vector $\mathbf{s}_{bk} = (s_{bk,1}, \ldots, s_{bk,L})^{\mathrm{T}}$, where T denotes vector transpose. An active user's pilot is transmitted over L signal dimensions in the coherence block. Each user is assigned a unique sequence and users' sequences are non-orthogonal, as assigning orthogonal pilot sequences is not feasible in mMTC with limited channel coherence time [7]. Users' pilot sequences in each cell are generated from independent and identically distributed (i.i.d) complex Gaussian distribution with zero-mean and unit-variance [5], denoted by $\mathcal{CN}(0, \mathbf{I}_L)$.

We assume that channels follow block-fading model, i.e., a channel coefficient between a user and its designated base station stays constant during each coherence block, which is made up of L signal dimensions in time and/or frequency. Channel coefficients vary among different blocks. Let $\mathbf{h}_{bjk}$ be the M-dimensional channel vector (i.e., small-scale channel fading coefficients) between user k in cell b and base station j. Similarly, Let g_{bjk} be the large-scale fading coefficient (LSFC), which includes path-loss, between user k in cell b and base station j. Let $a_{bk} \in \{0, 1\}$ be a binary variable, with $a_{bk} = 1$ indicating that the k-th user in cell b is active. Accordingly, the received uplink signal at the b-th base station can be modeled as

$$\begin{aligned}\mathbf{Y}_b &= \sum_{k=1}^{N} a_{bk}\mathbf{s}_{bk}g_{bbk}\mathbf{h}^{\mathrm{T}}_{bbk} + \sum_{j\neq b}\sum_{k=1}^{N} a_{jk}\mathbf{s}_{jk}g_{bjk}\mathbf{h}^{\mathrm{T}}_{bjk} + \mathbf{Z}_b, \\ &= \left[\mathbf{S}_1 \ldots \mathbf{S}_B\right]\begin{bmatrix}\mathbf{A}_1 & & \\ & \ddots & \\ & & \mathbf{A}_B\end{bmatrix}\begin{bmatrix}\mathbf{G}^{\frac{1}{2}}_{b1} & & \\ & \ddots & \\ & & \mathbf{G}^{\frac{1}{2}}_{bB}\end{bmatrix}\begin{bmatrix}\mathbf{H}_{b1} \\ \vdots \\ \mathbf{H}_{bB}\end{bmatrix} + \mathbf{Z}_b, \quad (2)\end{aligned}$$

where $\mathbf{S}_j = [\mathbf{s}_{j1}, \ldots, \mathbf{s}_{jN}]$ is the $L \times N$ matrix of pilot sequences of the users in cell j, $\mathbf{A}_j = \mathrm{diag}\{a_{j1}, \ldots, a_{jN}\}$ is a $N \times N$ diagonal matrix consisting of the binary user activity pattern in cell j, $\mathbf{G}_j = \mathrm{diag}\{g_{bj1}, \ldots, g_{bjN}\}$ denotes $N \times N$ diagonal matrix consisting of the LSFCs between the users in cell j and base station b, $\mathbf{H}_{bj} = [\mathbf{h}_{bj1}, \ldots, \mathbf{h}_{bjN}]^T$ is the Rayleigh fading channel between the users in cell j and base station b, and $\mathbf{Z}_b$ is additive white Gaussian noise (AWGN) that follows $\mathbf{Z}_b \sim \mathcal{CN}(0, \sigma^2\mathbf{I}_M)$ with variance σ^2.

The transmitted signals of all active users are collectively received at the central unit, through all B base stations, to jointly detect the user activity across all B cells. Then, the $L \times BM$ received signal $\tilde{\mathbf{Y}}$ at the central unit is expressed as

$$\begin{aligned}\tilde{\mathbf{Y}} &= \left[\mathbf{Y}_1 \ldots \mathbf{Y}_B\right] \\ &= \left[\mathbf{S}_1 \ldots \mathbf{S}_B\right]\begin{bmatrix}\mathbf{A}_1 & & \\ & \ddots & \\ & & \mathbf{A}_B\end{bmatrix}\begin{bmatrix}\mathbf{G}^{\frac{1}{2}}_{11}\mathbf{H}_{11} \ldots & \mathbf{G}^{\frac{1}{2}}_{B1}\mathbf{H}_{B1} \\ \vdots & \ddots \quad \vdots \\ \mathbf{G}^{\frac{1}{2}}_{1B}\mathbf{H}_{1B} \ldots & \mathbf{G}^{\frac{1}{2}}_{BB}\mathbf{H}_{BB}\end{bmatrix} \\ &\quad + \left[\mathbf{Z}_1 \ldots \mathbf{Z}_B\right]. \quad (3)\end{aligned}$$

We assume that the channel vectors $\{\mathbf{h}_{bjk} : k \in \mathcal{K}_c\}$ are spatially white and independent of each other (i.e., un-

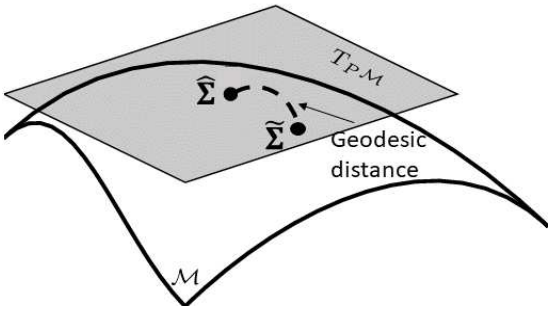

Fig. 2: Geodesic distance between the sample $\hat{\mathbf{\Sigma}}$ and estimated $\tilde{\mathbf{\Sigma}}$ covariance matrices on Riemannian manifold.

correlated along antennas) and are characterized by complex Gaussian distribution with zero-mean and identity-covariance, that is $\mathbf{h}_{bjk} \sim \mathcal{CN}(0, \mathbf{I}_{BM})$. Hence, the columns of $\tilde{\mathbf{Y}}$ in (3) are i.i.d Gaussian vectors with $\tilde{\mathbf{Y}}_{:,i} \sim \mathcal{CN}(0, \mathbf{\Sigma})$, where

$$\mathbf{\Sigma} = \sum_{b=1}^{B}\sum_{k=1}^{N} \gamma_{bk}\mathbf{s}_{bk}\mathbf{s}_{bk}^{\mathrm{H}} + \sigma^2\mathbf{I}_L, \tag{4}$$

represents the $L \times L$ covariance matrix, and is common among all the columns $\tilde{\mathbf{Y}}_{:,i}, i = \{1, \ldots, BM\}$. In (4), $\gamma_{bk} = a_{bk}\sqrt{g_{bk}}$ and it equals to $\gamma_{bk} = \sqrt{g_{bk}}$ for active users (i.e, $a_{bk} = 1$).

III. Problem Formulation over Riemannian Manifolds

In this section, we formulate the problem of detecting the binary variables $\{a_{bk}\}_{k=1}^{N}, b = 1,\ldots, B \in \{0, 1\}$, which represent the user activity pattern across all B cells. Such problem formulation can be done by considering both the sample and estimated covariance matrices of the received signals as follows. On one hand, the $L \times L$ sample covariance matrix of the columns of the received signal $\tilde{\mathbf{Y}}$ in (3) is

$$\hat{\mathbf{\Sigma}} = \frac{1}{BM}\tilde{\mathbf{Y}}\tilde{\mathbf{Y}}^{\mathrm{H}} = \frac{1}{BM}\sum_{i=1}^{BM}\tilde{\mathbf{Y}}_{:,i}\tilde{\mathbf{Y}}_{:,i}^{\mathrm{H}}, \tag{5}$$

which is a sufficient statistics to identify user activity [3], [5]. On the other hand and assuming $\{\hat{a}_{bk}\}_{k=1}^{N}, b = 1,\ldots, B \in \{0, 1\}$ to be the estimated user activity pattern across B cells, then the $L \times L$ estimated covariance matrix is expressed as

$$\tilde{\mathbf{\Sigma}} = \sum_{b=1}^{B}\sum_{k=1}^{N} \hat{a}_{bk}\mathbf{s}_{bk}\mathbf{s}_{bk}^{\mathrm{H}} + \sigma^2\mathbf{I}_L. \tag{6}$$

The sample $\hat{\mathbf{\Sigma}}$ and the estimated $\tilde{\mathbf{\Sigma}}$ covariance matrices are SPD ones, which can be represented over Riemannian manifolds as shown in Fig. 2. Consequently, the Log-determinant Bregman divergence, given in (1), can be used to measure the geodesic distance between such two covariance matrices. Hence, the activity detection problem can reformulated as finding the estimated users' activity vector $\hat{a}_{bk}$, and hence the estimated covariance matrix $\tilde{\mathbf{\Sigma}}$ in (6), by minimizing the Log-determinant Bregman divergence objective function as

$$\min_{\hat{a}_k} \mathcal{D}_g(\hat{\mathbf{\Sigma}} \| \tilde{\mathbf{\Sigma}}) = -\log\det\hat{\mathbf{\Sigma}} + \log\det\tilde{\mathbf{\Sigma}} + \langle\langle \tilde{\mathbf{\Sigma}}^{-1}, \hat{\mathbf{\Sigma}} - \tilde{\mathbf{\Sigma}} \rangle\rangle. \tag{7}$$

The lower the estimation error, or difference in (7), the lower the probability of miss detection in the users' activity.

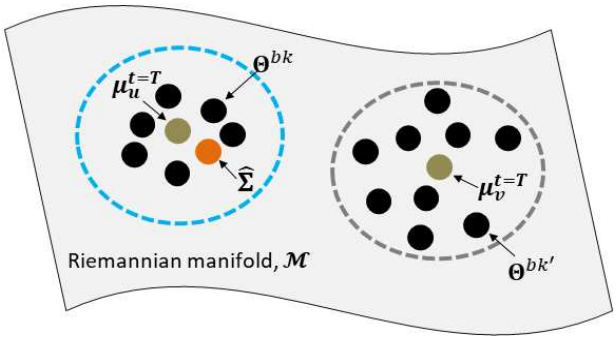

Fig. 3: Proposed geometric k-means clustering approach for users' activity detection over Riemannian manifolds.

IV. Learning Users' Activity Pattern in mMIMO Multi-Cell System Via Geometric k-Means Clustering over Riemannian Manifolds

The objective of this section is to estimate the binary users' activity pattern $\{\hat{a}_{bk}\}_{k=1}^{N}, b=1,\ldots, B$, which minimizes the objective function in (7). To this end, we propose a geometric k-means approach that divides the users into two clusters, i.e., active and inactive users. In doing so, users are geometrically represented over Riemannian manifold and the inter-user geometric distance is measured via the geodesic one (i.e., log-determinant Bregman divergence). Intuitively, the k-means clustering creates two clusters with far-apart centroids as follows. The first cluster combines the set of active users, and its centroid represents the estimated covariance matrix $\tilde{\mathbf{\Sigma}}$ in (6). It approaches the sample covariance matrix $\hat{\mathbf{\Sigma}}$ in (5), which satisfies the minimization problem in (7). On the contrary, the centroid of the inactive users' clusters is relatively far apart from sample covariance matrix $\hat{\mathbf{\Sigma}}$ in (5).

Fig. 3 illustrates the learning mechanism of the proposed activity detection solution. We define the inputs of the proposed clustering model to be a set of BN users' signatures. The users' signatures are represented over Riemannian manifolds (black dots in Fig. 3), through the received sample covariance matrix $\hat{\mathbf{\Sigma}}$ and the user's pilot sequences $\{\mathbf{s}_{bk}\mathbf{s}_{bk}^{\mathrm{H}}\}_{k=1}^{N}, b = 1,\ldots,B$, and they are given by

$$\left\{\mathbf{\Theta}^{bk}\right\}_{k=1}^{N} = \left\{\left(\hat{\mathbf{\Sigma}} - \mathbf{s}_{bk}\mathbf{s}_{bk}^{\mathrm{H}}\right) + \alpha\mathbf{I}_L\right\}_{k=1}^{N}, b=1,\ldots,B, \tag{8}$$

where $\mathbf{\Theta}^{bk}$ is an $L \times L$ positive definite matrix by adding an identity matrix $\mathbf{I}_L$ and $\alpha > 0$ is a regularization parameter. As shown in (8), the pilot sequence of any active user is subtracted from the sample covariance matrix $\hat{\mathbf{\Sigma}}$, which in fact contains that user's pilot sequence. In contrast, inactive users' pilots are not included in the sample covariance matrix $\hat{\mathbf{\Sigma}}$. Intuitively, such contract enables the K-means clustering to distinguish between the two groups of users. In summary and as illustrated in Fig. 3, the clustering mechanism uses the set of users' signatures $\left\{\mathbf{\Theta}^{bk}\right\}_{k=1}^{N}\ \forall b$, and matches one of the cluster centroids (green dots in Fig. 3) to the sample covariance matrix $\hat{\mathbf{\Sigma}}$ (orange dots in Fig. 3) to find the representations of the active users (black dots inside blue circle in Fig. 3) over Riemannian manifolds.

Algorithm 1 Psuedo-Code of proposed learning-based model for user activity detection in multi-cell systems.

1: **Inputs:** $\{\boldsymbol{\Theta}^{bk} \in \mathcal{S}_{++}^{n}\}_{k=1}^{N}, b=1,\ldots,B, \hat{\boldsymbol{\Sigma}}$;
2: **Outputs:** User activity pattern;
3: **Initialization:** $\{\mathscr{C}_v^{(t=0)}\}_1^2 = \emptyset$ and number of cluster set as 2;
4: **Initialization:** Randomly choose two SPDs from $\{\boldsymbol{\Theta}^{bk}\}$ as the
5: cluster means $\mu_1^{(t=0)}$ and $\mu_2^{(t=0)}$;
6: **repeat**
7: **for** $b = 1, \ldots, B$ **do**
8: **for** $k = 1, \ldots, N$ **do**
9: $\mathscr{C}_v^{(t)} = \{\boldsymbol{\Theta}_v^{bk} | \mathcal{D}(\boldsymbol{\Theta}_v^{bk}, \mu_v^{(t)}) \leq \mathcal{D}(\boldsymbol{\Theta}_v^{bk}, \mu_u^{(t)})\}, \forall v, u; v \neq u, 1 \leq u \leq 2$
10: **end for**
11: **for** $v = 1, 2$ **do**
12: $\mu_v^{(t+1)} = \underset{p \in \mathcal{S}_{++}^{n}}{\operatorname{argmin}} \frac{1}{|\mathscr{C}_v^{(t)}|} \sum_{u \in \mathscr{C}_v^{(t)}} \mathcal{D}^2(p, \boldsymbol{\Theta}_u^{bk}), 1 \leq u \leq 2$
13: **end for**
14: **end for**
15: **until** convergence
16: **if** $\mathcal{D}_1(\hat{\boldsymbol{\Sigma}}, \mu_1^{(t=T)}) < \mathcal{D}_2(\hat{\boldsymbol{\Sigma}}, \mu_2^{(t=T)})$ **then**
17: $\mathscr{C}_1^{(t=T)}$ is selected as a group of active users;
18: **else**
19: $\mathscr{C}_2^{(t=T)}$ is selected as a group of active users;
20: **end if**
21: **return** $\{\hat{a}_{bk}\}_{k=1}^{N}, b=1,\ldots,B \in \{0,1\}$;

The complete solution is described in Algorithm 1 as follows. The *inputs* to Algorithm 1 are the SPD matrices from set $\{\boldsymbol{\Theta}^{bk} \in \mathcal{S}_{++}^{n}\}_{k=1}^{N}$, $b=1,\ldots,B$ (line 1) and the *outputs* are the estimated user activation pattern $\{\hat{a}_{bk}\}_{k=1}^{N}, b = 1,\ldots,B$. During the initialization phase, both sets of cluster class assignments are set to an empty set $\{\mathscr{C}_v^{(t=0)}\}_1^2 = \emptyset$ and the number of desired clusters is set to two as part of the clustering process (line 3). The next step is to initialize the cluster centroids, denoted by $\mu_1^{(t)}$ and $\mu_2^{(t)}$, by randomly selecting two SPDs from $\{\boldsymbol{\Theta}^{bk} \in \mathcal{S}_{++}^{n}\}_{k=1}^{N}$, $b=1,\ldots,B$ (lines 4-5).

The proposed algorithm assigns each observation $\boldsymbol{\Theta}^{bk}$ to one of the two clusters based on the smallest geodesic distance (i.e., log-determinant Bregman divergence) to their centers (lines 8-10). Then it updates the cluster centroids by Fréchet mean [16] of each cluster (lines 11-13), until the cluster assignment converges. When the algorithm converges, in other words, centroids are no longer updated, the algorithm stops running and produces two sets of clusters.

Next, the algorithm classifies the two clusters into active users and inactive ones as follows. The cluster with the minimum log-determinant Bregman divergence between its centroid $\mu_{v\in\{1,2\}}^{t=T}$ and sample covariance matrix $\hat{\boldsymbol{\Sigma}}$ is selected as one with the active users (lines 16-17). Whereas, the other one is assigned to include inactive users (lines 18-19). In other words, the k-means clustering model sttempts to match one of the cluster centroids to the sample covariance matrix $\hat{\boldsymbol{\Sigma}}$ to find the signatures of the active users over Riemannian manifolds. Then, it produces the user activation pattern $\{\hat{a}_{bk}\}_{k=1}^{N}, b=1,\ldots,B$ across all B cells by finding the indices of the corresponding users' signatures in the cluster with active users (line 21).

V. Performance Evaluation

In this section, we present the simulation results of the proposed geometric clustering solution and compare it against other Euclidean-based state-of-the-art solutions.

A. Simulation Setup

In this paper, we consider a multi-cell system consisting $B = 3$ circular cells (as considered in [5]) where the radius of each cell is 1000m and potential users are uniformly distributed throughout the cells. Among these, the ratio of active users to the total users is set as 0.1 per cell. The number of antennas of each base station is set as $M = 45$ and the pilot sequence $\mathbf{s}_{bk}$ of each user with length L have i.i.d. entries and is generated from a complex Gaussian distribution with zero-mean and unit-variance, as explained in Section II-B.

The LSFC is modeled as $128.1 + 37.6\log_{10}(d)$, where d is the distance between the base station and the user in kilometers. The background noise power spectrum density is -169 dBm/Hz over 10 MHz, and each device transmitted power is set to 25 dBm. For fair comparsion, the simulation parameters are kept the same as in [3], [4].

We consider probability of miss detection P_{md} as the performance metric in this paper. The probability of miss detection correspond to the event that a user is active but declared inactive. We define $\hat{\mathcal{K}}_c$ as the estimate of the set of active users, derived from the output of the learned user activity pattern $\{\hat{a}_{bk}\}_{k=1}^{N}, b=1,\ldots,B$ by Algorithm 1. Then the probability of miss detection P_{md} can be expressed as

$$P_{md} = \frac{\mathbb{E}[|\, \mathcal{K}_c \cap \hat{\mathcal{K}}_c \,|]}{K_c}, \tag{9}$$

where $\mathcal{K}_c$ and K_c denote the set of true active users and the total number of true active users across B cells, respectively. Also, $\mathbb{E}$ represents the averaging over all sources of randomization including users' locations and Rayleigh-fading channels.

B. Simulation Results

To show the effectiveness of the proposed Riemannian clustering method, we first consider a special case of single-cell scenario (i.e., $B = 1$) and compare it with other covariance-based state-of-the-art solutions, such as multiple measurement vector (MMV) in [3] and coordinate-wise descent algorithm (CDA) in [4], which do not consider multiple cells. Then, we introduce the inter-cell interference in multi-cell scenario and demonstrate the benefit of exploiting multi-cell cooperation in the proposed Riemannian clustering method.

1) Single-Cell Scenario: In the single-cell scenario, we first validate that the proposed method minimizes objective function (7) by presenting Fig. 4 with $M = 45$, $K_c = 40$. In particular, we substitute the estimated user activity patterns $\{\hat{a}_{bk}\}_{k=1}^{N}, b = 1,\ldots,B$ of MMV [3], CDA [4], and the proposed method in (6) to find the estimated covariance matrix $\tilde{\boldsymbol{\Sigma}}$. Then, we calculate the log-determinant Bregman divergence between the sample $\hat{\boldsymbol{\Sigma}}$ and estimated $\tilde{\boldsymbol{\Sigma}}$ covariance matrices for different pilot sequence lengths L. As shown in Fig. 4, the proposed clustering method has the lowest log-determinant Bregman divergence compared to MMV [3] and CDA [4].

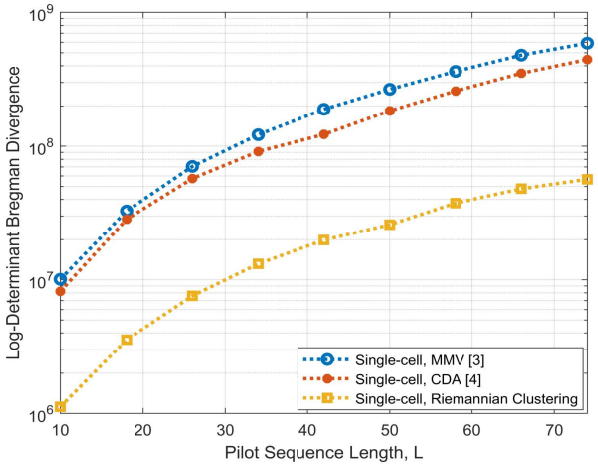

Fig. 4: Log-Determinant Bregman Divergence in (7) for different pilot sequence length L in single-cell scenario.

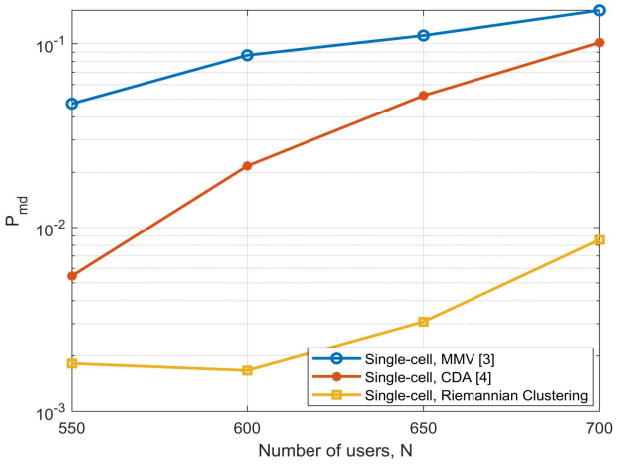

Fig. 6: Probability of miss detection with different number of users N in single-cell scenario.

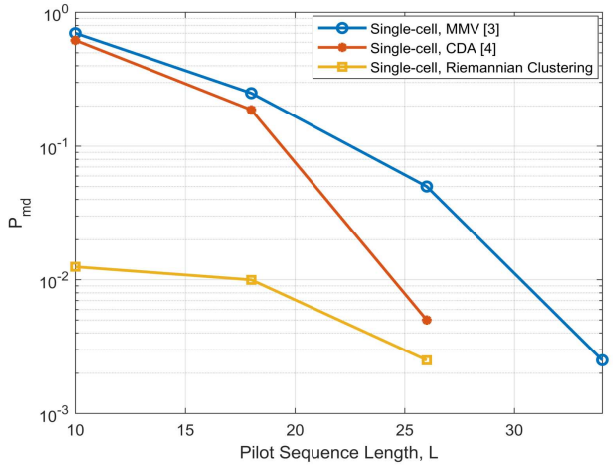

Fig. 5: Probability of miss detection with different pilot sequence length L in single-cell scenario.

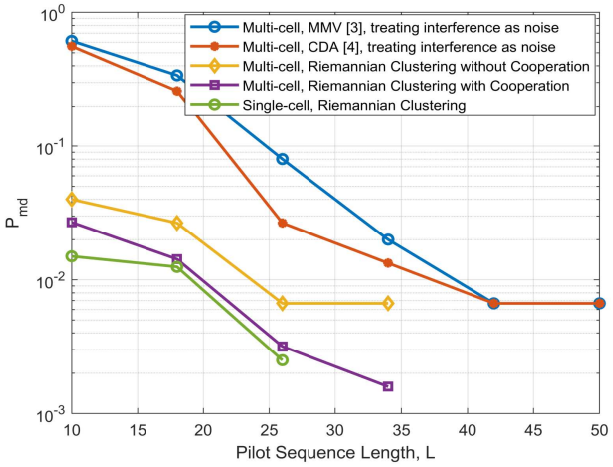

Fig. 7: Probability of miss detection with different pilot sequence length L in the multi-cell scenario.

The probability of miss detection is shown in Fig. 5 for the proposed other covariance-based solutions, as the pilot sequence length L increases. As can be observed, increasing the pilot sequence length L leads to a substantial reduction in probability of miss detection, and the proposed clustering model outperforms both MMV [3] and CDA [4]. Such results are in agreement with the ones in Fig. 4, as lower log-determinant Bregman divergence between the sample covariance matrix $\hat{\mathbf{\Sigma}}$ and the estimated one $\tilde{\mathbf{\Sigma}}$ leads to lower probability of miss detection.

The probability of miss detection changes with the number of users N, as presented in Fig. 6, with $M = 45$ and $L = 35$, while keeping the ratio of active users to the total users fixed at 0.1. As shown in Fig. 6, the probability of miss detection increases as N increases for all of the covariance-based detection approaches. However, the proposed k-Means clustering method exhibits the lowest probability of miss detection values compared to the MMV [3] and CDA [4].

2) Multi-Cell Scenario: We evaluate the performance of two different approaches for multi-cell scenario, which are a) cooperative approach and b) non-cooperative approach. The cooperative approach was previously presented in Section IV, where cooperation among the multiple cells is incorporated in the clustering mechansim. In the non-cooperative approach, no cooperation among the cells is considered. Particularly, each base station operates independently to detect the user activation in its own cell, while treating inter-cell interference as noise. The sample and estimated covariance matrices are formed independently for activity detection in each cell.

Fig. 7 illustrates the probability of miss detection of the proposed clustering approach with $M = 45$, $N = 300$, $K_c = 30$, and different pilot lengths L. As shown, when no cooperation is considered, the probability of miss detection of the proposed approach decreases under inter-cell interference, as compared to the performance in a single-cell scenario. However with cooperation, the proposed method achieves very close probability of miss detection to the single-cell scenario.

Besides, the proposed clustering approach significantly outperforms generalized multi-cell versions of MMV [3] and CDA [4], in which inter-cell interference is treated as noise.

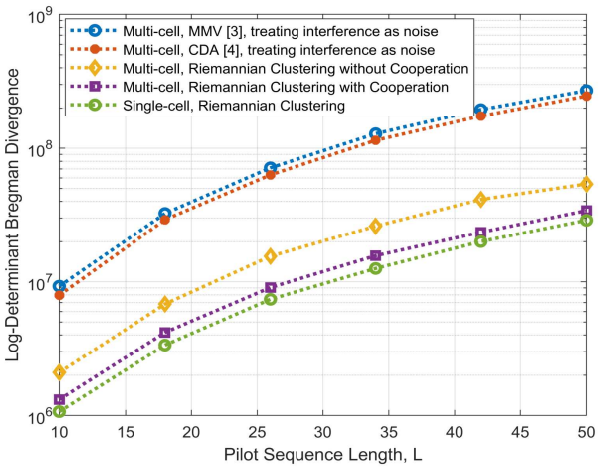

Fig. 8: Log-Determinant Bregman Divergence in (7) for different pilot sequence length L in in multi-cell scenario.

For instance at $L = 26$, the proposed approach achieves 96% and 88% reduction of probability of miss detection as compared to the MMV [3] and CDA [4], respectively.

Finally, Fig. 8 shows the log-determinant Bregman Divergence between the sample covariance $\hat{\mathbf{\Sigma}}$ and estimated covariance $\tilde{\mathbf{\Sigma}}$ by various activity detection strategies in the multi-cell scenario. As shown in Fig. 8, the proposed cooperative Riemannian clustering method has the lowest log-determinant Bregman divergence than MMV [3], CDA [4], and the non-cooperative one in multi-cell settings. Similar to the single-cell scenario, this result illustrates that the lower log-determinant Bregman divergence leads to lower probability of miss detection, as was shown in Fig. 7.

C. Computational Complexity

The computational complexity of the proposed geometric k-means clustering model (as in Algorithm 1) is $\mathcal{O}(TBNkL)$, where T is the total number of iterations to converge, B is the total number of cells, N denotes the total number of users, and k is the desired number of clusters. As shown, the complexity of the proposed approach is *linear* in the pilot length L, due to simple distance measurements and averaging over distances as done in lines 9 and 12 of Algorithm 1), respectively. As the number of cells and clusters are set at 3 and 2, respectively, the computational complexity of proposed method is $\mathcal{O}(2T3NL) \approx \mathcal{O}(TNL)$. On the other hand, the computational complexity of both MMV [3] and CDA [4] is $\mathcal{O}(\tilde{T}NL^2)$, where $\tilde{T}$ is the total number of iterations to converge. Hence, the complexity of Euclidean-based solutions is *quadratic* in L due to matrix-vector multiplications used in coordinate-wise descent algorithm. Hence, the proposed clustering approach over Riemannian (i.e., non-Euclidean) manifolds requires less computational complexity compared to Euclidean-based ones (e.g., MMV [3] and CDA [4].)

VI. Conclusion

In this paper, we have proposed a cooperative users' activity detection approach over Riemannian manifolds for multi-cell massive MIMO systems. In doing so, users' unique signatures were represented over Riemannian manifolds using a combination of the sufficient-statistic sample covariance matrix and user-dependent pilot sequences. Consequently, geometric k-means clustering was applied over Riemannian manifolds to partition the users' signatures into two groups, active and inactive users. Simulation results have demonstrated that the proposed clustering approach over Riemannian manifolds has achieved above 88% reduction in the probability of miss detection compared to Euclidean-based state-of-the-art ones, and was effective in both single-cell and multi-cell scenarios. Finally and along with achieving lower miss detection probability, the proposed non-Euclidean approach requires less complexity compared to its Euclidean counterparts.

References

[1] Q. Lin, Y. Li and Y. -C. Wu, "Sparsity Constrained Joint Activity and Data Detection for Massive Access: A Difference-of-Norms Penalty Framework," in IEEE Transactions on Wireless Communications, vol. 22, no. 3, pp. 1480-1494, March 2023.

[2] K. Senel and E. G. Larsson, "Grant-Free Massive MTC-Enabled Massive MIMO: A compressive sensing approach," IEEE Trans. Commun., vol. 66, no. 12, pp. 6164–6175, Dec. 2018.

[3] S. Haghighatshoar, P. Jung and G. Caire, "Improved Scaling Law for Activity Detection in Massive MIMO Systems," 2018 IEEE International Symposium on Information Theory (ISIT), Vail, CO, USA, 2018.

[4] Z. Chen, F. Sohrabi, Y. -F. Liu and W. Yu, "Covariance Based Joint Activity and Data Detection for Massive Random Access with Massive MIMO," ICC 2019 - 2019 IEEE International Conference on Communications (ICC), Shanghai, China, 2019.

[5] Z. Chen, F. Sohrabi and W. Yu, "Sparse Activity Detection in Multi-Cell Massive MIMO Exploiting Channel Large-Scale Fading," in IEEE Transactions on Signal Processing, vol. 69, pp. 3768-3781, 2021.

[6] X. Shao, X. Chen, D. W. K. Ng, C. Zhong, and Z. Zhang, "Cooperative Activity Detection: Sourced and Unsourced Massive Random Access Paradigms," IEEE Trans. Signal Process., vol. 68, pp. 6578–6593, Nov. 2020, https://ieeexplore.ieee.org/document/9266124.

[7] U. K. Ganesan, E. Björnson and E. G. Larsson, "Clustering-Based Activity Detection Algorithms for Grant-Free Random Access in Cell-Free Massive MIMO," in IEEE Transactions on Communications, vol. 69, no. 11, pp. 7520-7530, Nov. 2021, doi: 10.1109/TCOMM.2021.3102635.

[8] A. S. Ibrahim, "Rethinking Maximum Flow Problem and Beamforming Design Through Brain-inspired Geometric Lens," GLOBECOM 2020 - 2020 IEEE Global Communications Conference, Taipei, Taiwan, 2020.

[9] R. Shelim and A. S. Ibrahim, "Wireless Link Scheduling Over Recurrent Riemannian Manifolds," in IEEE Transactions on Vehicular Technology, vol. 72, no. 4, pp. 4959-4968, April 2023.

[10] R. Shelim and A. S. Ibrahim, "Learning Wireless Power Allocation Through Graph Convolutional Regression Networks Over Riemannian Manifolds," in IEEE Transactions on Vehicular Technology, vol. 73, no. 3, pp. 3652-3662, March 2024, doi: 10.1109/TVT.2023.3325200.

[11] I. Nasim and A. S. Ibrahim, "Relay Placement for Maximum Flow Rate via Learning and Optimization Over Riemannian Manifolds," in IEEE Transactions on Machine Learning in Communications and Networking, vol. 1, pp. 197-209, 2023, doi: 10.1109/TMLCN.2023.3309772.

[12] M.P. do Carmo, "Differential Geometry of Curves and Surfaces: Revised and Updated Second Edition", Dover Books on Mathematics. Dover Publications, 2016.

[13] J. M. Lee, "Introduction to Riemannian Manifolds", Springer, 2018.

[14] L. M. Bregman, "The Relaxation Method for Finding the Common Point of Convex Sets and its Application to the Solution of Problems in Convex Programming", USSR Computational Mathematics and Mathematical Physics, 7:191–204, 1967. MR0215617

[15] P. Ravikumar, M. J. Wainwright, G. Raskutti, B. Yu. "High-Dimensional Covariance Estimation by Minimizing l1-penalized Log-Determinant Divergence." Electronic Journal of Statistics, 5(none) 935-980 2011.

[16] K. You, H.-J. Park, "Re-Visiting Riemannian Geometry of Symmetric Positive Definite Matrices for the Analysis of Functional Connectivity", NeuroImage, Volume 225, 2021, 117464, ISSN 1053-8119.